Acta Crystallographica Section F
Structural Biology and Crystallization Communications
ISSN 1744-3091

Pedro M. Matias,[a]* Jana Tatur,[b] Maria Arménia Carrondo[a] and Wilfred R. Hagen[b]

[a]Instituto de Tecnologia Química e Biológica, Universidade Nova de Lisboa, Av. República, EAN, 2784-505 Oeiras, Portugal, and [b]Department of Biotechnology, Delft University of Technology, Julianalaan 67, 2628 BC Delft, The Netherlands

Correspondence e-mail: matias@itqb.unl.pt

Received 11 February 2005
Accepted 13 April 2005
Online 22 April 2005

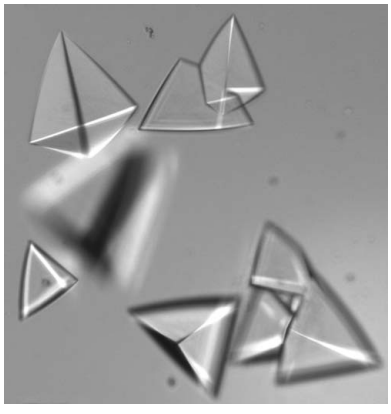

Crystallization and preliminary X-ray characterization of a ferritin from the hyperthermophilic archaeon and anaerobe *Pyrococcus furiosus*

Crystals of the title protein have been produced and preliminary structural analysis has been carried out. The crystals belong to the orthorhombic space group $C222_1$, with unit-cell parameters a = 258.1, b = 340.1, c = 266.5 Å. The protein forms a 24-mer of 20 kDa subunits, which assemble with 432 non-crystallographic symmetry. A total of 36 monomers are found in the asymmetric unit, corresponding to one and a half 24-mers.

1. Introduction

Ferritin is the generic name for a class of small (∼20 kDa) helical proteins that ubiquitously occur in the three domains of life, both in aerobic and anaerobic cells. Ferritins spontaneously polymerize into a 24-meric hollow sphere-like structure (inner diameter 8 nm and outer diameter 12 nm), which can be homopolymeric or, in higher eukaryotes, can be made up of two (H and L) (Crichton, 2001) or three (H, L, M) homologous subunits (Ha *et al.*, 1999). A ferritin homologue known as Dps (for DNA-protecting protein during starvation) forms smaller hollow spheres (inner diameter $\simeq$ 4.5 nm and outer diameter $\simeq$ 9 nm) as 12-mers (Grant *et al.*, 1998). Ferritins are thought to function physiologically as reversible stores of iron (and possibly of oxoanions and of other metal ions) and/or as protecting systems against oxidative damage of cell components, notably DNA (Smith, 2004). Ferritins can be viewed as enzymes as they catalyze the oxidation of Fe^{II} and the formation of a Fe^{III} mineral core in their interior. Each subunit carries a ferroxidase active centre consisting of a μ-oxo bridged dinuclear iron cluster. Proteins from the subclass of bacterioferritins additionally have heme groups sandwiched between two subunits, presumably functioning in electron transfer (Stiefel & Watt, 1979). In recent years, interest in ferritins has increased remarkably in view of their putative technological application in nanoscience, environmental remediation, fuel cells and magnetic information storage (Hosein *et al.*, 2004; Sleytr *et al.*, 1999; Zhang *et al.*, 2000).

Here, we report the crystallization and preliminary structure analysis of *Pf*Ftn, the ferritin from *Pyrococcus furiosus*. *P. furiosus* is a marine strictly anaerobic fermentative hyperthermophilic archaeon with an optimal growth temperature of 373 K. A putative ferritin gene has been cloned and overexpressed in *Escherichia coli* and the purified protein is an active non-heme ferritin forming a 24-meric structure that can incorporate up to 2700 Fe ions (as determined by chemical analysis) into a superparamagnetic core when incubated with Fe^{II} under air. This protein exhibits the highest thermostability known among ferritins: its core-formation activity is fully retained after incubation at 373 K for 8 h or autoclaving at 393 K for 20 min (our unpublished results). While a number of crystallographic structures are available for ferritins, bacterioferritins and Dps from several species (Carrondo, 2003), archaeal structural data are limited to a ferritin from the sulfate-reducing thermophile *Archaeoglobus fulgidus* (PDB code 1sq3; Johnson *et al.*, 2005) and a Dps-like ferritin from the mesophilic halophile *Halobacterium salinarum* (PDB codes 1tjo, 1tk6, 1tko, 1tkp; Zeth *et al.*, 2004). In *A. fulgidus* ferritin, a novel 23 symmetry was found, which opens four large pores through which it may be possible for large molecules to enter the protein (Johnson *et al.*, 2005). Contrarily, in the current study on *P. furiosus* ferritin

(*Pf*Ftn) the more common quaternary structure among ferritins with 432 non-crystallographic symmetry was observed, indicating that the 23 symmetry found in *A. fulgidus* is not a general trait among archaeal ferritins. The high thermostability of *Pf*Ftn will probably be explained from structural data. The mechanism of iron incorporation into ferritins is under debate. In the hyperthermophilic *Pf*Ftn, pre-steady-state kinetics of iron uptake can be slowed drastically at ambient temperatures (our unpublished results), which may allow following of the iron-incorporation pathway in protein crystals.

2. Experimental procedures and results

2.1. Protein production

P. furiosus DSM 3638 cells were grown as described in Arendsen *et al.* (1995). Genomic DNA was isolated with sodium dodecyl sulfate and sodium lauryl sarcosine, and extraction was performed with phenol/chloroform/isoamylalcohol (Sambrook *et al.*, 1989). The putative ferritin gene was PCR-amplified using 5 ng of genomic DNA, 15 pmol of each primer (forward primer 5′-CCATATGTT-GAGCGAAAGAATGC-3′ and reverse primer 5′-GTCGACTTA-CTCTCCTCCCTG-3′), 15 nmol dNTPs, 50 nmol $MgSO_4$ and 1.25 U of *Pfx* polymerase in a total volume of 50 µl. The PCR program consisted of a melting step at 368 K for 5 min followed by 30 cycles of 368 K for 1 min, 329 K for 1 min and 345 K for 1.5 min and a final extension step at 345 K for 10 min. The amplified gene was cloned into pCR 2.1-TOPO vector (Invitrogen). The fidelity of the ferritin gene-containing clone was confirmed by DNA sequencing (Base-Clear). The plasmid pCR 2.1-TOPO was isolated with QIA Spin miniprep Kit (Qiagen), restriction-digested with *Nde*I and *Sal*I (Roche) and cloned into the same restriction sites of the vector pET24a(+) (Novagen). The resulting clone was transformed into competent *E. coli* DH5α-T1^{R} cells (Invitrogen). The construct produced was expressed in BL21-CodonPlus (DE3)-RIL cells (Stratagene). The pre-culture of the transformed cells was cultivated aerobically at 310 K and 200 rev min^{-1} in 100 ml LB medium (Sambrook *et al.*, 1989), 50 µg ml^{-1} chloramphenicol and 20 µg ml^{-1} kanamycin overnight. The pre-culture was transformed in TB medium (Sambrook *et al.*, 1989) in a 1:20 ratio for 2 h and induced with 1 m*M* IPTG. The cells were harvested by centrifugation after an additional 5 h of growth. The cells were washed in 20 m*M* Tris–HCl buffer pH 8 and DNase, RNase and 0.5 m*M* PMSF were added. The cells were broken with a Cell Disruptor (Constant Systems). The cell-free extract was subjected to heat treatment (353 K, 10 min) and clarified by centrifugation. The supernatant was loaded onto a HiLoad Superdex 200 26/60 column (Amersham Biosciences) equilibrated with 20 m*M* Tris–HCl buffer pH 8 and 0.15 *M* NaCl. The fractions exhibiting ferroxidase activity were pooled and concentrated (Amicon, YM-100).

2.2. Iron incorporation and determination

Ferritin iron loading was performed by adding a freshly and anaerobically prepared aqueous solution of iron sulfate containing 0.1% HCl to a solution of apoferritin in 50 m*M* HEPES pH 7 under aerobic conditions.

Core-formation activity was monitored at 315 nm using $\varepsilon = 2200\ M^{-1}\ cm^{-1}$ (Bonomi *et al.*, 1996)

Iron in the protein samples was determined based on the methods of Hennessy *et al.* (1984) and Pierik *et al.* (1992) by chelating it with ferrene and reading the absorption of the iron–ferrene complex at 593 nm, $\varepsilon = 35\ 500\ M^{-1}\ cm^{-1}$.

2.3. Crystallization

Crystals of *Pf*Ftn were produced aerobically using the hanging-drop vapour-diffusion method at room temperature. Commercially available screens (Crystal Screen 1 and SaltRx, Hampton Research) were used for crystallization screening. The best crystals were obtained with 2 *M* ammonium sulfate (Crystal Screen 1, solution 32; Fig. 1). Further optimization attempts by varying the pH and concentration of ammonium sulfate and the concentration of the protein did not produce better crystals. Several other crystallization conditions produced small crystals, spherulites or needles. Optimization of those conditions was attempted by seeding or factorial experiments, but did not lead to any improvement of the results. The crystals used for data collection were grown against 0.5 ml of 2 *M* ammonium sulfate reservoir solution, with drops containing 2 µl of 5 mg ml^{-1} protein solution in 50 m*M* HEPES pH 7 and an equal amount of the reservoir solution. The crystals of the 'as isolated' ferritin, containing ∼17 Fe atoms per 24-mer, grew in three weeks

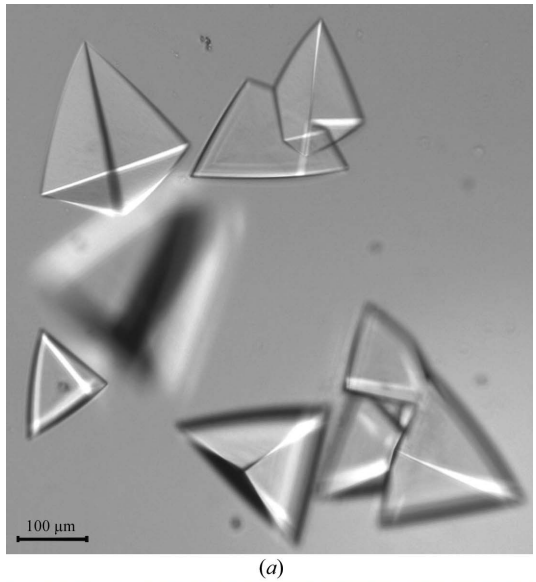

(*a*)

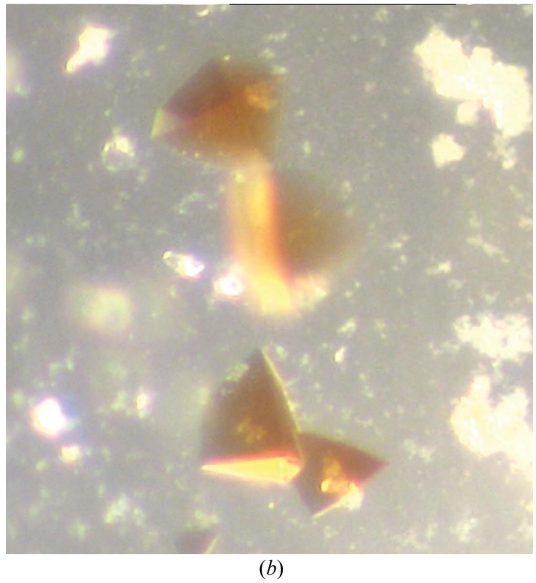

(*b*)

Figure 1
Crystals of *P. furiosus* ferritin. (a) 'As isolated', ∼17 Fe atoms per 24-mer. (*b*) Iron-containing ferritin, ∼1000 Fe atoms per 24-mer. The colour of the iron-loaded protein solution and crystals prepared from it depends on the amount of iron loaded and varies from light yellow to brown.

and those loaded with ∼1000 Fe atoms per 24-mer (as estimated from the amount of loaded iron prior to crystallization) in four months. The crystals exhibited pyramidal shapes with base side and height of 150–250 µm (Fig. 1).

2.4. X-ray data collection and preliminary crystallographic analysis

Cryoprotecting conditions were established in-house and consisted of briefly dipping the crystals into a modified crystallization solution containing 20% glycerol prior to flash-freezing them at 110 K in a nitrogen-gas stream using an Oxford Cryosystems low-temperature device.

Diffraction data from an 'as-isolated' *Pf*Ftn crystal were collected at ESRF beamline ID14-2 from a single flash-frozen crystal at 100 K. The diffraction images were integrated with the program *MOSFLM* (Leslie, 1992). The processed data were scaled, merged and converted to structure factors using the *CCP*4 program suite (Collaborative Computational Project, Number 4, 1994). Data-processing statistics are summarized in Table 1. The diffraction data obtained is not very strong [$I/\sigma(I)$ = 5.4 overall], consistent with the relatively high merging R factor (0.115 for data to 3.0 Å). In addition, the scaling results revealed signs of crystal decay arising from radiation damage in the X-ray beam after only little more than 6–7 min exposure to the beam. Fine φ-slicing (0.25°) was also necessary during data collection in order to minimize spatial overlaps on the detector surface, owing to the unfavourable orientation of the crystal in the loop, with the longest cell axis, c, making a 38° angle with the spindle.

A loaded *Pf*Ftn crystal with ∼1000 Fe atoms per 24-mer was also tested on the X-ray beam. However, this crystal was smaller and diffraction could only be observed to about 6 Å.

Cell-volume considerations led to the conclusion that there might be between one and three 24-mers in the asymmetric unit, corresponding to values of V_M (Matthews, 1968) between 6.1 and 2.0 Å^3 Da^{-1}, with an estimated solvent content ranging between 80 and 39%.

The self-rotation Patterson maps (Fig. 2) show peaks consistent with 432 point-group symmetry, typical of a 24-mer quaternary arrangement for the ferritins.

2.5. Structure determination by molecular replacement

The determination of the three-dimensional structure of *Pf*Ftn was undertaken by the molecular-replacement (MR) method using the program *PHASER* (Storoni *et al.*, 2004) and the homologous ferritin from the thermophilic bacterium *Thermotoga maritima* (PDB code 1vlg) as the search model. The sequence of this 164-amino-acid ferritin has 89 amino-acid residues identical with that of *Pf*Ftn (174 amino acids), corresponding to 51% homology, and the only insertions or deletions occur at the termini of the protein chains. The MR calculations were carried out using the standard *PHASER* protocol as implemented through the *CCP*4 graphical user interface, with reflection data to 3.2 Å resolution. Because no strong peaks were observed in a Patterson map calculated using the native *Pf*Ftn diffraction data, there was no indication of any translational symmetry between 24-mers in the asymmetric unit and therefore in the first *PHASER* calculation only one 24-mer was considered as the search model. Indeed, the self-rotation function indicated that one or more of the fourfold NCS rotation axes in the 24-mer might be parallel or even coincident with a crystallographic twofold axis. Therefore, it was assumed that two 12-mers (each corresponding to half of a 24-mer) might be present in the asymmetric unit, fulfilling this condition. In each case, the second half of the 24-mer would then be generated by the corresponding crystallographic twofold rotation. The 12-mer search model was constructed from the published structure coordinates of the ferritin from *T. maritima*. The MR

Table 1
X-ray diffraction data-collection and processing statistics.

Values in parentheses refer to the last resolution shell, 3.16 ≥ d ≥ 3.00 Å.

Beamline	ESRF ID14-EH2
Detector	ADSC Quantum 4
Wavelength (Å)	0.933
Space group	$C222_1$
Unit-cell parameters (Å)	
a	258.1
b	340.1
c	266.5
Resolution range (Å)	83.3–3.0
No. observations	731509
No. unique reflections	225192
Completeness (%)	97.4 (98.8)
Redundancy	3.2 (3.2)
R_{merge}†	0.115 (0.316)
$I/\sigma(I)$	5.4 (2.3)
Estimated $B_{overall}$ (Å^2)	60.2

† $R_{merge} = \sum_{hkl}\sum_i |I_{hkl,i} - \langle I_{hkl}\rangle| / \sum_{hkl}\sum_i |I_{hkl,i}|$, where $\langle I_{hkl}\rangle$ is the mean intensity of the set of symmetry-related reflections denoted by $I_{hkl,i}$.

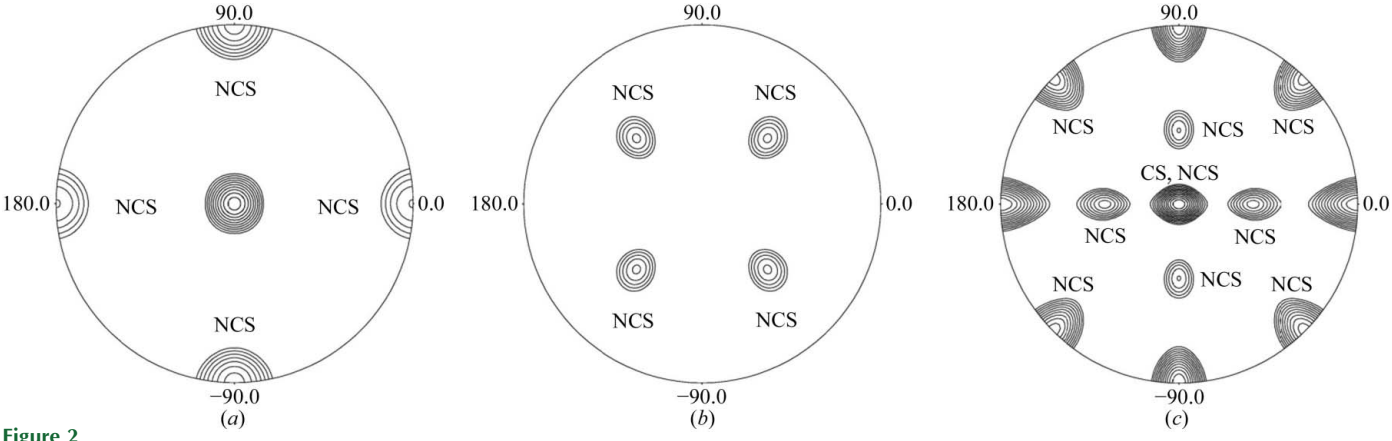

Figure 2
Self-rotation Patterson function plots for *Pf*Ftn in the resolution range 3.5 ≤ d ≤ 15 Å with integration range 5 ≤ R ≤ 20 Å. Peaks in the sections shown at κ = 90° (*a*), κ = 120° (*b*) and κ = 180° (*c*) give the orientation of the crystallographic twofold and non-crystallographic twofold, threefold and fourfold (NCS) rotation axes in the crystal structure. The maximum value was normalized to 100 and the contours drawn at five-unit intervals, starting at 40. Drawings were prepared with programs *POLARRFN*, *NPO* and *XPLOT84DRIVER* (Collaborative Computational Project, Number 4, 1994).

calculations with *PHASER* gave a strong solution, but inspection of crystal packing on a three-dimensional graphics workstation revealed that the search model was incomplete. Only one of the 24-mers was actually found to be lying on a crystallographic twofold axis along cell edge *b*. Another 24-mer is located in general positions, of which only half was accounted for by the search model. The *PHASER* calculations were repeated using the two previously located 12-mer positions to look for the missing 12-mer. A single solution was found, with *Z* score 86.5, which completed the model. The second-best solution, with *Z* score 74.9, was rejected owing to C^{α} clashing. The asymmetric unit of the *Pf*Ftn crystal structure was therefore found to contain one and a half 24-mers (36 monomers). It is interesting to note that the 24-mer that lies in a special position, with one of its NCS fourfold axes coincident with a crystallographic twofold axis along cell edge *b*, has the other two orthogonal NCS fourfolds slightly misaligned with the other two crystallographic unit-cell directions. On the other hand, the 24-mer lying in general positions has its NCS fourfold axes slightly ($\sim$10°) offset from those of the first 24-mer. This arrangement explains the lack of a strong peak in the native Patterson map arising from non-crystallographic translation symmetry between the 24-mers, which should be present if the NCS fourfold axes from both 24-mers were exactly parallel, as in the case of bacterioferritin from *Desulfovibrio desulfuricans* ATCC 27774 (Coelho *et al.*, 2001). Furthermore, it also explains the differences observed in the intensity of the peaks in the self-rotation Patterson maps which arise from the NCS symmetry twofold and fourfold rotation axes (see Fig. 2), since the observed pattern results from the combination of two 432 NCS patterns, one from each 24-mer, which are slightly misaligned with respect to each other.

Despite the success of the MR calculations, we believe that because of the low resolution of the diffraction data and low homology of the search model, as well as the complexity of the structure, experimental phase information is needed in order to obtain the best possible structural model from the data. To that end, a MAD experiment at the Fe *K* absorption edge will be carried out at the earliest opportunity.

The authors wish to thank the ESRF (Grenoble, France) for financial and technical support during data collection.

References

Arendsen, A. F., Veenhuizen, P. T. & Hagen, W. R. (1995). *FEBS Lett.* **368**, 117–121.
Bonomi, F., Kurtz, D. M. & Cui, X. (1996). *J. Biol. Inorg. Chem.* **1**, 67–72.
Carrondo, M. A. (2003). *EMBO J.* **22**, 1959–1968.
Coelho, A. V., Macedo, S., Matias, P. M., Thompson, A. W., LeGall, J. & Carrondo, M. A. (2001). *Acta Cryst.* D**57**, 326–329.
Collaborative Computational Project, Number 4 (1994). *Acta Cryst.* D**50**, 760–763.
Crichton, R. R. (2001). *Inorganic Biochemistry of Iron Metabolism: From Molecular Mechanisms to Clinical Consequences.* Chichester: John Wiley & Sons.
Grant, R. A., Filman, D. J., Finkel, S. E., Kolter, R. & Hogle, J. M. (1998). *Nature Struct. Biol.* **5**, 294–303.
Ha, Y., Shi, D., Small, G. W., Theil, E. C. & Allewell, N. M. (1999). *J. Biol. Inorg. Chem.* **4**, 243–256.
Hennessy, D. J., Reid, G. R., Smith, F. E. & Thompson, S. L. (1984). *Can. J. Chem.* **62**, 721–724.
Hosein, H. A., Strongin, D. R., Allen, M. & Douglas, T. (2004). *Langmuir*, **20**, 10283–10287.
Johnson, E., Cascio, D., Sawaya, M. R., Gingery, M. & Schröder, I. (2005). *Structure*, **13**, 637–648.
Leslie, A. G. W. (1992). *Jnt CCP4/ESF–EACBM Newsl. Protein Crystallogr.* **26**.
Matthews, B. W. (1968). *J. Mol. Biol.* **33**, 491–497.
Pierik, A. J., Wolbert, R. B., Mutsaers, P. H., Hagen, W. R. & Veeger, C. (1992). *Eur. J. Biochem.* **206**, 697–704.
Sambrook, J., Fritsch, E. F. & Maniatis, T. (1989). *Molecular Cloning: A Laboratory Manual.* Cold Spring Harbor, NY, USA: Cold Spring Harbor Laboratory Press.
Sleytr, U. B., Messner, P., Pum, D. & Sára, M. (1999). *Angew. Chem. Int. Ed.* **38**, 1034–1054.
Smith, J. L. (2004). *Crit. Rev. Microbiol.* **30**, 173–185.
Stiefel, E. I. & Watt, G. D. (1979). *Nature (London)*, **279**, 81–83.
Storoni, L. C., McCoy, A. J. & Read, R. J. (2004). *Acta Cryst.* D**60**, 432–438.
Zeth, K., Offermann, S., Essen, L. O. & Oesterhelt, D. (2004). *Proc. Natl Acad. Sci. USA*, **101**, 13780–13785.
Zhang, N., Fengyi, L., Fu, Q. J. & Tsang, S. C. (2000). *React. Kinet. Catal. Lett.* **71**, 393–404.